Proceedings of DSCC2008
2008 ASME Dynamic Systems and Control Conference
October 20-22, 2008, Ann Arbor, Michigan, USA

DSCC2008-2238

EXPERIMENTAL CALIBRATION AND VALIDATION OF FAULT DIAGNOSIS AND PROGNOSIS ALGORITHMS FOR AUTOMOTIVE ELECTRIC POWER GENERATION AND STORAGE SYSTEM

Weiwu Li
Center for Automotive Research and
Department of Electrical Engineering
The Ohio State University
li.779@osu.edu

Chris Suozzo
Center for Automotive Research and
Department of Electrical Engineering
The Ohio State University
suozzo.2@osu.edu

Simona Onori
Center for Automotive Research
The Ohio State University
onori.1@osu.edu

Giorgio Rizzoni
Center for Automotive Research and
Department of Mechanical Engineering
The Ohio State University
rizzoni.1@osu.edu

Mutasim A. Salman
General Motors
Electrical & Controls Integration Lab
mutasim.a.salman@gm.com

Frank Zhang
General Motors
Electrical & Controls Integration Lab
(Currently with
Wright State University)
xiaodong.zhang@wright.edu

ABSTRACT
This paper is a continuation of the work on the model-based fault diagnosis for the automotive electric power generation system (EPGS) presented in [5]. Based on the previous work on the subject, a new and optimized fault diagnosis algorithm for the EPGS system is developed. In this paper, the thresholds for the diagnosis algorithm are selected and calibrated based on experimental data. The test bench used for the calibration and validation process is discussed. Finally the effectiveness of the fault diagnosis algorithm and threshold selection is validated using experimental data collected from the test bench.

NOMENCLATURE

V_f	Alternator field voltage	[V]
V_{ref}	Alternator reference voltage	[V]
V_{dc}	Alternator voltage	[V]
I_{dc}	Alternator current	[A]
I_f	Alternator field current	[A]
R_f	Field winding resistance	[Ω]
L_{ff}	Field winding self inductance	[H]
ω_e	Electrical frequency	[rad/s]
θ_e	Electrical angle	[rad]
M	Mutual inductance between field and phase	[H]
Vbatt	Battery voltage	[V]
Iload	load current	[A]
Idc_eq	Alternator current output from equivalent model	[A]
Vdc_eq	Alternator voltage output from equivalent model	[V]
Vf_eq	Field voltage output from equivalent model	[A]

INTRODUCTION
The modern vehicles are highly dependent on the operation of the electrical power generation, storage and distribution system. Especially with the potential safety-relevant X-by-wire system application, it is essential to have a reliable diagnosis of the electrical power generation and storage system. It will be extremely helpful to give an early warning to the user when the EPGS system leaves its safe operating area due to whatever reasons. Meanwhile, such a capability will also improve resource management via condition-based maintenance, and minimize the operational costs for vehicle owners. However, as the complexity of the electrical systems has increased, there is a concomitant increased difficulty in the identification of the malfunction phenomena (subsystem failure modes, ambiguity caused by cross-subsystem failure propagation).

The first section of this paper describes the newly updated and optimized system simulation model and the fault diagnosis algorithm. Then the test bench used for the calibration and validation process is introduced. The threshold selection and calibration process is then discussed. Finally, a complete experimental validation example is given.

SYSTEM SIMULATION MODEL AND FAULT DIAGNOSIS ALGORITHM

The EPGS system is composed of an alternator and a battery, while all the other electrical or electronic sub-systems are lumped into one current sink as shown by Figure 1.

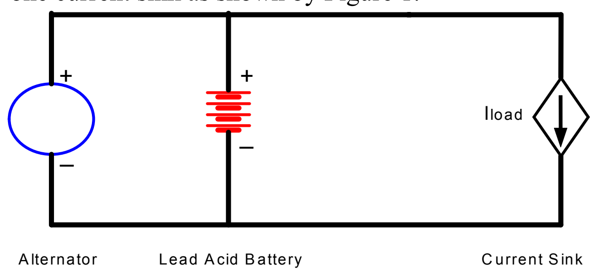

FIGURE 1. SIMPLIFIED EPGS SYSTEM DIAGRAM.

EPGS System Simulation Model

A reliable simulation model for the EPGS system is essential for understanding the system dynamics and for further conducting fault diagnosis. To make the EPGS simulation model more accurate and flexible for the purpose of fault diagnosis, we modified and optimized the EPGS model used in [5]. The common automotive claw-pole alternator structure can be described by Figure 2.

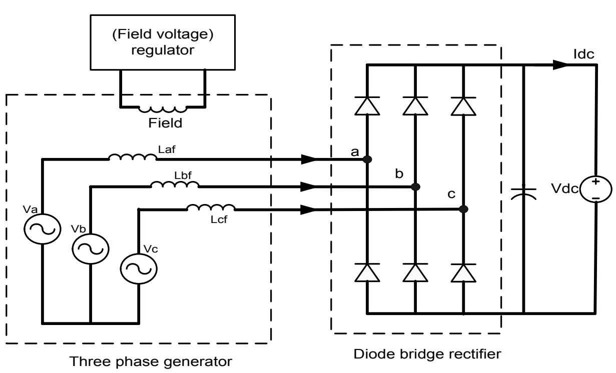

FIGURE 2. AUTOMOTIVE ALTERNATOR STRUCTURE.

In the modified alternator simulation model, the SimPowerSystems library of Simulink is used together with Simulink itself to simulate the whole EPGS model. The SimPowerSystems is a module-based power system simulation tool available in Matlab. It can be combined seamlessly with analytical equation to realize the simulation of complex systems. A big advantage of utilizing the SimPowerSystems in the EPGS simulation is the possibility of simulating the diode bridge rectifier subsystem, and this provides extreme flexibility and convenience for the simulation of diode fault.

In the EPGS system simulator, the alternator stator, the rectifier, the battery and the load model are implemented and embedded in the SimPowerSystems, as illustrated in Figure 3.

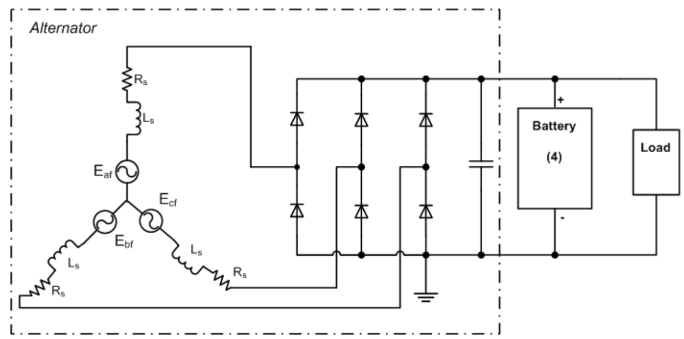

FIGURE 3. SIMPOWER SUB-SYSTEMS.

The schematic of the final EPGS system model is shown in Figure 4. The controller, excitation field and field induced EMF are described by the equations shown below.

Controller:

$$V_f = K_P \cdot \left(V_{ref} - V_{dc}\right) + K_I \cdot \int \left(V_{ref} - V_{dc}\right) \cdot dt \qquad (1)$$

Where the field voltage V_f is saturated at V_{dc}.

Excitation field:

$$\dot{i}_f = \frac{1}{L_{ff}} \cdot V_f - \frac{R_f}{L_{ff}} \cdot I_f - \frac{1}{L_{ff}} \cdot \left(\frac{\mathbf{d}}{\mathbf{d}\theta_e} \mathbf{L}_\mathbf{f}^\mathrm{T}(\theta_e) \cdot \omega_e \cdot \mathbf{I} + \mathbf{L}_\mathbf{f}^\mathrm{T}(\theta_e) \cdot \dot{\mathbf{I}} \right) \qquad (2)$$

where

$$\mathbf{I} = \begin{pmatrix} I_a \\ I_b \\ I_c \end{pmatrix}; \quad \mathbf{L}_\mathbf{f}(\theta_\mathbf{e}) = \begin{pmatrix} L_{af}(\theta_e) \\ L_{bf}(\theta_e) \\ L_{cf}(\theta_e) \end{pmatrix} = \begin{pmatrix} M \cdot \cos(\theta_e) \\ M \cdot \cos(\theta_e - \Phi) \\ M \cdot \cos(\theta_e + \Phi) \end{pmatrix}$$

$$\Phi = \tfrac{2}{3}\pi$$

Field induced EMF:

$$\mathbf{E}_\mathbf{f} = \frac{\mathbf{d}}{\mathbf{d}\theta_e} \mathbf{L}_\mathbf{f}(\theta_e) \cdot \omega_e \cdot I_f + \mathbf{L}_\mathbf{f}(\theta_e) \cdot \dot{i}_f \qquad (3)$$

where

$$\mathbf{E}_\mathbf{f} = \begin{pmatrix} E_{af} \\ E_{bf} \\ E_{cf} \end{pmatrix}.$$

As in [5], the serpentine belt slip fault, rectifier diode open fault and voltage regulator fault are considered as system faults. The belt slip fault is an input fault that occurs when the alternator belt does not have the proper tension to keep the alternator pulley rotating synchronously with the engine shaft; it may be caused by the aging of the serpent belt or wrong installation. The effect of this fault is a decrease in alternator output voltage, which the voltage regulator compensates for by increasing the field voltage. The power electronics fault consists of a failure of one of the bridge rectifier diodes, causing that part of the branch to be open. Characteristics of this fault include: a large ripple in the output voltage and current. The voltage regulator fault consists of an error in the reference voltage that also produces a reduction or increase of output alternator voltage and current. Those faults can be easily implemented by changing one parameter or breaking one diode. The fault injection is also illustrated in Figure 4.

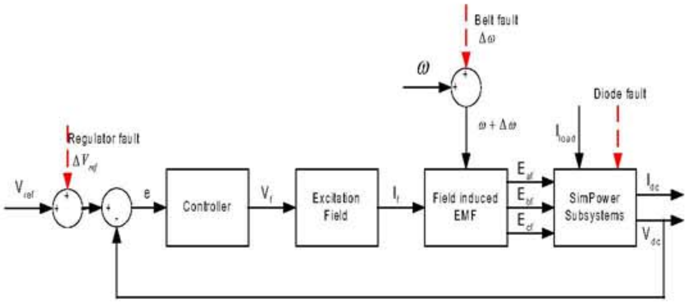

FIGURE 4. EPGS SIMULATION MODEL SCHEME.

Fault diagnosis algorithm

Model-based fault detection and isolation (FDI) is predicated on the ability to construct residual generators based on models of the system (for example, through the design of state observers or parity equations). Unfortunately, the complexity of the EPGS system is significant.

For the alternator system, the combination of the nonlinear dynamics of the three-phase generator with the switched, state-dependent behaviour of the diode bridge rectifier, make the design of such residual generators very challenging. Linearization is, for example, virtually impossible in the presence of the hard nonlinearities in the rectifier. Meanwhile, a direct nonlinear parity equation or observer design for such a complex non-linear switch system will also be extremely difficult. In [1], the authors present several complicated nonlinear sliding model observer methods for alternator EMF estimation. However, those methods are dependent on the availability of alternator phase current which is not available.

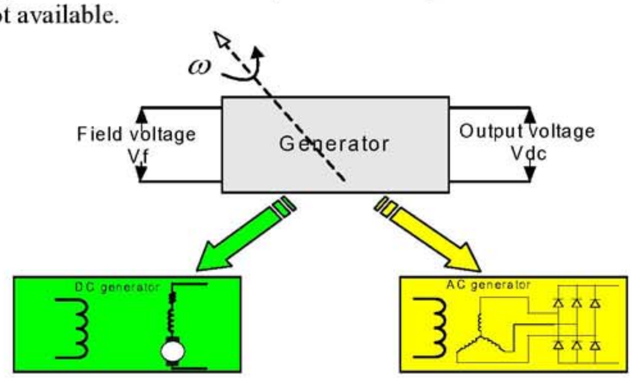

FIGURE 5. INPUT-OUTPUT PERSPECTIVE OF AN ALTERNATOR.

In order to obtain a robust diagnosis algorithm, and in light of its implementation in the vehicle, our approach utilizes an equivalent alternator model based on the input-output relationship. Figure 5 describes the input-output relationship in the alternator system which is the starting point for the identification of an equivalent DC generator model for the alternator. The equivalent representation is made possible by the replacement of the AC synchronous generator and diode bridge rectifier from the nonlinear model with an equivalent DC generator. To increase the accuracy of the equivalent model, the equivalent model is identified and interpolated at different working zones. A comprehensive description of this equivalent model can be found in [2, 3].

The designed fault diagnosis algorithm uses a parity equation approach. The approach is based on the equivalent model and it compares the behaviour of the alternator with the behaviour of the equivalent model to produce the residuals that contain the information of the faults. The diagnosis residuals are defined in Table 1. The fault diagnosis process can be illustrated by Figure 6.

TABLE 1. FAULT DIAGNOSIS RESIDUALS

Residual	Definition
r_1	*(Idc – Idc_eq)/Idc_nom*
r_2	*(Vf – Vf_eq)/Vref_nom*
r_3	*(Vdc – Vdc_eq)/Vref_nom*

In Table 1, *Idc_nom* is the nominal alternator current, which is chosen as 120 [A]; *Vref_nom* is the nominal reference voltage, which is chosen as 14.46 [V].

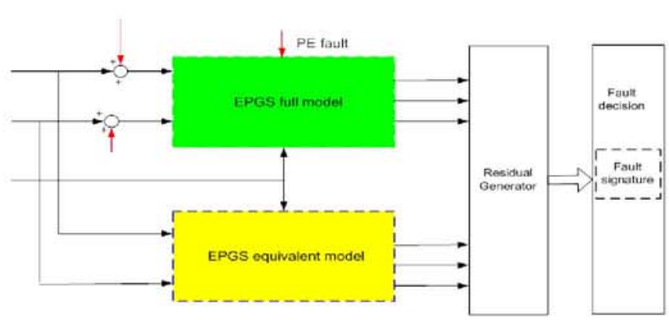

FIGURE 6. MODEL-BASED FAULT DIAGNOSIS SCHEME.

It is important to notice that the equivalent model is used as an open loop estimator for the full model without fault. The behaviour of the equivalent model is not affected by any faults. After a fault effect analysis exploiting the equivalent model, the fault signature and fault isolation strategy is given by equation (4) and Table 2, respectively.

Fault signature are decided by

$$sig\_r_1 = \begin{cases} 1, & std(r_1) > h_1 \\ 0, & std(r_1) < h_1 \end{cases}$$

$$sig\_r_2 = \begin{cases} 1, & mean(r_2) > h_2 \\ 0, & mean(r_2) < h_2 \end{cases} \quad (4)$$

$$sig\_r_3 = \begin{cases} 1, & mean(r_2) > h_{3\_up} \\ -1, & mean(r_2) < h_{3\_down} \\ 0, & else \end{cases}$$

In equations (4), *std*() stands for the standard deviation function over a time period, *mean*() stands for the average function over a time period, and in TABLE 2, the sign X indicates " don't care".

TABLE 2. FAULT ISOLATION LOGIC

	No fault	Rectifier fault	Regulator fault (Vref increase)	Regulator fault (Vref drop)	Belt slip fault
Sig_r1	0	1	0	0	0
Sig_r2	0	X	X	0	1
Sig_r3	0	X	1	-1	0/-1

It is worth mentioning that to decrease the false alarm which may be caused by noise or transient change of load current or engine speed, we used window-based averaging for the signature calculation. Such averaging reduces the effects of noise and modeling error on the detection, and therefore reducing the probability of false alarm.

EXPERIMENTAL TEST BENCH

The purpose of the test bench setup is to provide a reliable validation platform for the real electrical power generation system. The test bench can be used to imitate automotive EPGS environment, simulate component faults, and validate the EPGS fault diagnosis algorithms. The EPGS experimental test bench is located at Center for Automotive Research, OSU.

The automotive EPGS test bench is mainly composed of an electric motor, a vehicle alternator, a programmable power load and a 12 Volt lead-acid battery. The electric motor speed can be controlled by serial communication, so it is used to simulate the rotation performance of the engine. The programmable electric load is used to simulate the vehicle load demands by running a predefined load current profile. The electric load can also be remotely controlled by serial communication. The battery and the alternator works together to provide the current demanded by the load. Figure 7 shows the schematics of the EPGS test bench.

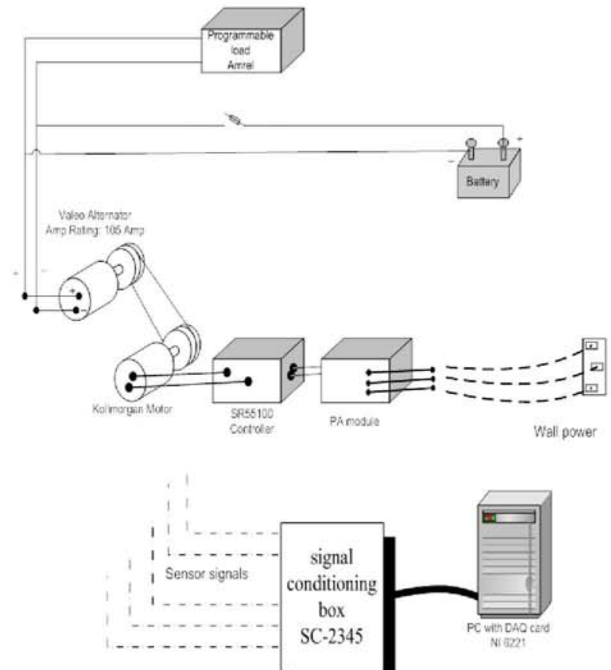

FIGURE 7. SCHEMATICS OF EPGS TEST BENCH.

The test bench DAQ system was developed on MATLAB DAQ toolbox; it provides a seamless linkage between data acquisition and data analysis in the MATLAB environment. The developed DAQ system is able to collect all signals of interest: Alternator voltage, alternator current, battery voltage, battery current, load current, motor RPM, alternator RPM and alternator field voltage. The DAQ system is also used to control the motor speed and electric load current level as programmed.

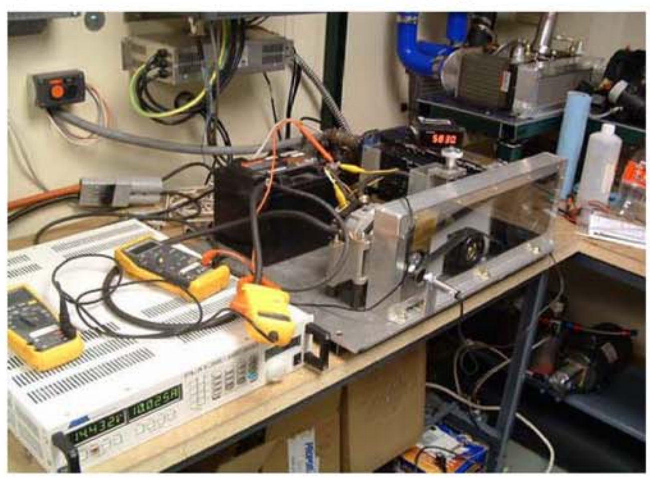

FIGURE 8. PART OF THE EPGS TEST BENCH SETUP AT CAR, OSU.

Faults Simulation by Test Bench

An important function of the test bench is to simulate EPGS faults which are encountered in real vehicles in order to validate the designed diagnosis algorithms. The simulation of two kinds of faults has been made possible on the test bench, which will be described next.

Rectifier Fault Simulation

A common fault with the alternator rectifier is a diode fault. The diode may be damaged by high voltage or other reasons. With the test bench, this kind of fault can be realized by cutting off the connection wire of one diode, as shown in Figure 9. For the convenience of operation, a manual switch can be added to the diode connection wire. So by turning on or off the switch, we can switch easily between no fault and diode fault condition.

FIGURE 9. RECTIFIER FAULT SIMULATION.

Belt Slip Fault Simulation

For the alternator belt slip fault simulation, a manually tunable idler is used between the alternator and the motor pulley. By adjusting the position of the idler, the tightness of the belt could be controlled precisely as shown in Figure 10.

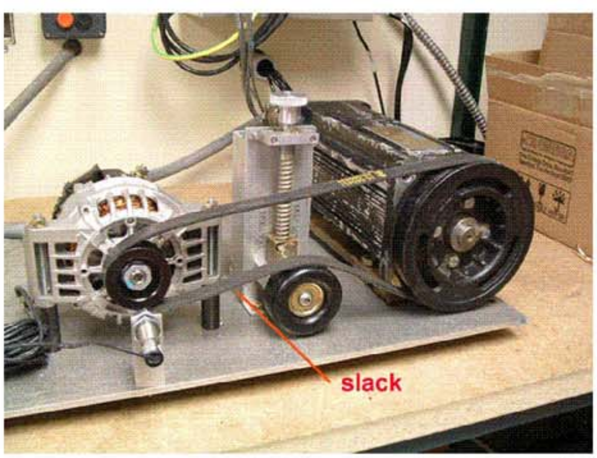

FIGURE 8. BELT SLIP FAULT SIMULATION.

THRESHOLD SELECTION AND CALIBRATION

Residual processing is a very important part of FDI scheme. In fact, because of model inaccuracy, disturbance or measurement noise, conditions for perfectly robust residual generation cannot be met in practice. Thus, it is important to be able to systematically design detection thresholds to make decisions from residuals. Optimal threshold selection based on statistical hypothesis testing is a commonly used threshold selection method.

Optimal Threshold Selection Method

The optimal threshold selection method is based on the statistical hypothesis testing concepts ([5]). In this method, residuals are viewed as a sequence of independent random variables. In a binary hypothesis test, residuals corresponding to normal operation are assumed to be randomly distributed under the hypothesis H_0 (no fault); residuals that correspond to a faulty condition are assumed to be randomly distributed under hypothesis H_1 (faulty). Let p_0 and p_1 be the probability density functions (*pdf*) corresponding to each probability distribution, as illustrated in Figure 11.

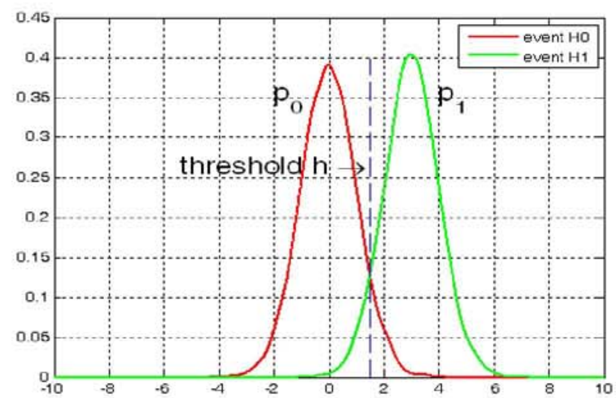

FIGURE 11. PDF OF RANDOM VARIABLE UNDER HYPOTHESIS H0 AND H1.

Let r be the random variable corresponding to a residual. The rule adopted most commonly is that whenever a sample of the random variable r is above the threshold value, we choose hypothesis H1, while we choose H0 if the sample is below the threshold. If the *pdf* associated with *r* under each hypothesis is known, we can compute various probabilities that are relevant in the context of fault diagnosis.

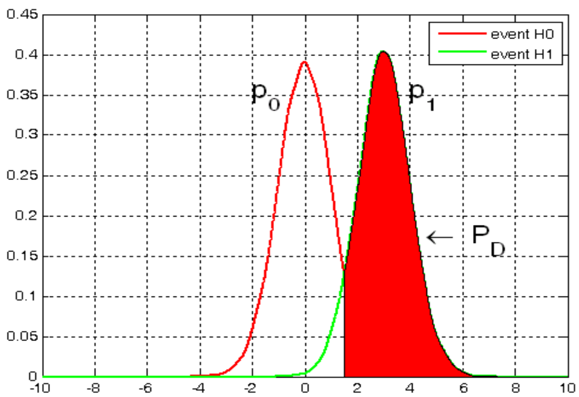

FIGURE 12. PROBABILITY OF DETECTION.

Probability of detection (P_D): the probability that we choose hypothesis H_1 when H_1 is indeed the correct hypothesis. It can be defined by

$$P_D = \int_h^{+\infty} p_1(x)dx \quad (5)$$

Where h is the selected threshold and p_1 is the *pdf* of the random variable r under hypothesis H_1. This probability is illustrated in Figure 12.

Probability of a false alarm (P_F): the probability that we choose hypothesis H_1 when H_0 is the correct hypothesis. It can be defined by

$$P_F = \int_h^{+\infty} p_0(x)dx \quad (6)$$

Where h is the selected threshold and p_0 is the *pdf* of the random variable r under hypothesis H_0. This probability is s illustrated in Figure 13.

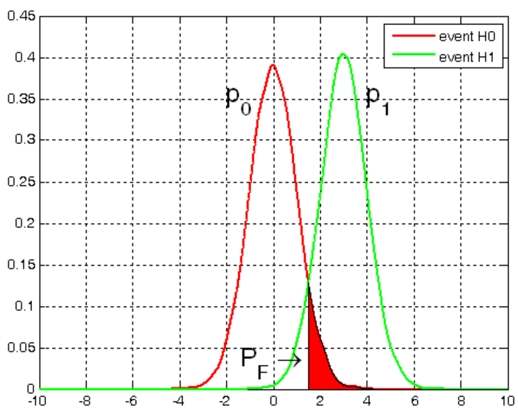

FIGURE 13. PROBABILITY OF FALSE ALARM.

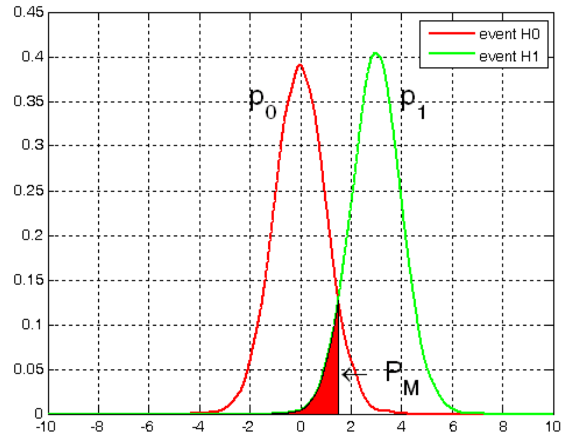

FIGURE 14. PROBABILITY OF MISDETECTION.

Probability of a misdetection (miss) (P_M): the probability that we choose hypothesis H_0 when H_1 is the correct hypothesis. It can be defined by

$$P_M = \int_{-\infty}^{h} p_1(x)dx \quad (7)$$

Where h is the selected threshold and p_1 is the *pdf* of the random variable r under hypothesis H_1. This probability is s illustrated in Figure 14.

Optimal threshold selection should result in P_D as high as possible and P_F and P_M as low as possible. However, these objectives are usually conflicting in real applications. Thus, the threshold selection problem is always a compromise between *misses* and *false* alarms. A practical but effective way to obtain the statistical optimal threshold is by minimizing the total probability of error ($P_F + P_M$).

Threshold Selection Results

From signature equation (4), there are four thresholds needed to be calibrated, where residual h_1 is related the belt slip fault, h_2 is related to the rectifier diode fault, h_{3_up} and h_{3_down} are related to the regulator fault. With the EPGS test bench, we are able to simulate the fault in the belt and in the rectifier. In this paper, we only calibrate threshold h_1 and h_2 while assuming that the pre-selected residual threshold h_{3_up} (0.04) and h_{3_down} (-0.04) are already acceptable.

To apply the threshold selection methods introduced before, an extensive numbers of experimental tests are conducted to generate the estimation of residual probability density function.

Threshold h_1 is selected by the statistical optimal threshold method and the final value is 0.053. It's shown in Figure 15.

Threshold h_2 is selected by the statistical optimal threshold method and the final value is 0.13. It's shown in Figure 16.

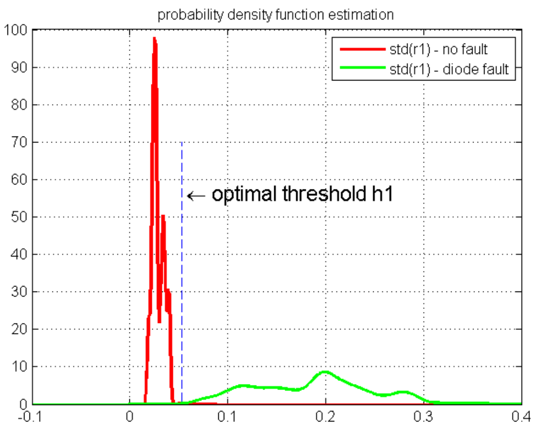

FIGURE 15. STATISTICAL OPTIMAL THRESHOLD H.

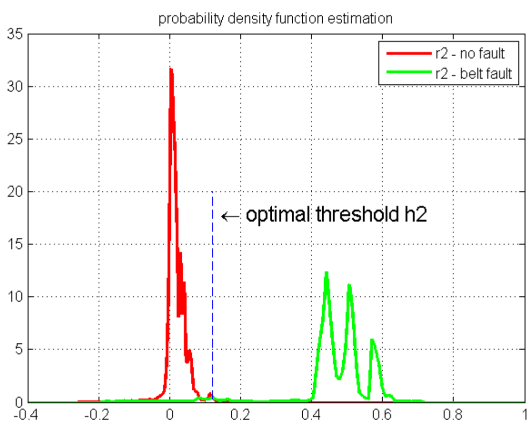

FIGURE 16. STATISTICAL OPTIMAL THRESHOLD H2.

VALIDATION EXAMPLE

After determining the threshold calibration, the effectiveness of EPGS diagnosis strategy and the selected threshold needs to be validated by experimental setup. The experimental validation of the fault diagnosis algorithm is carried out offline and is shown by Figure 17.

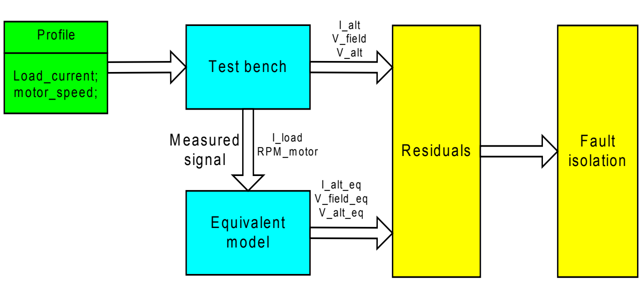

FIGURE 17. EXPERIMENTAL VALIDATION PROCESS.

A combined 180s experimental data is used as a diagnosis validation example. The input profile is composed of the three identical sections. Each section corresponds to different fault scenarios (see Figure 18). The input profiles are shown in Figure 18 and 19. At the first 60s, no fault happened; during 60s-120s, a short belt slip fault is introduced from 80s to 88s; from 120s-180s, the diode fault is injected on the whole period.

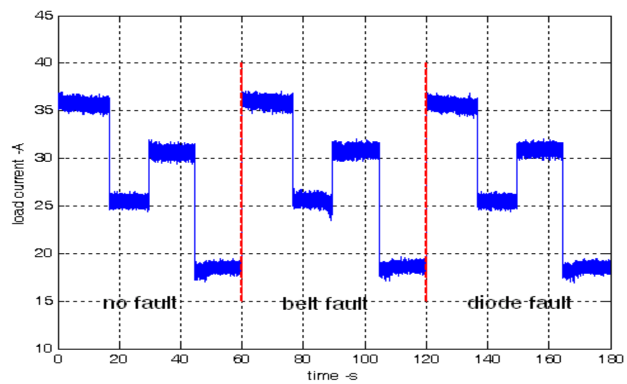

FIGURE 18. VALIDATION PROFILE – LOAD CURRENT

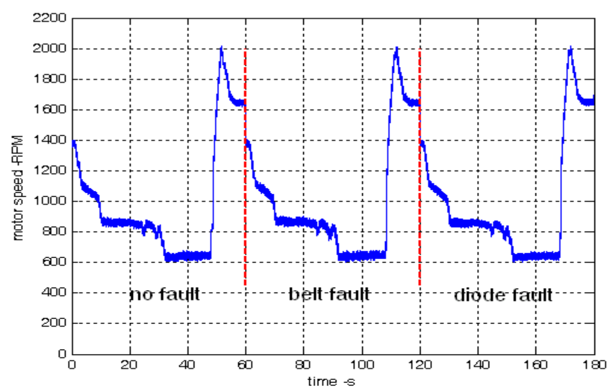

FIGURE 19. VALIDATION PROFILE – MOTOR SPEED.

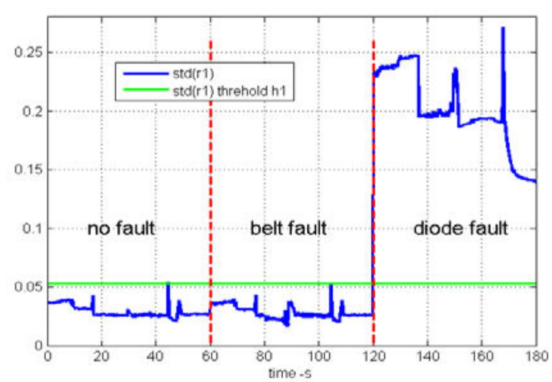

FIGURE 20. STANDARD DEVIATION OF RESIDUAL R1.

The generated fault residual is shown in Figure 20 to Figure 22, and the corresponding fault signature is shown in Figure 23 to

Figure 25. Checking with fault isolation logic Table 2, we can conclude that: at the first 60 seconds, no fault is detected; from 80s-89s, a belt slip fault is detected; and from 120s to 180s, diode fault is detected. The conclusions match exactly with the experimental setup. The correct fault detection and isolation of this validation shows the effectiveness of the fault diagnosis algorithm and threshold selection methods.

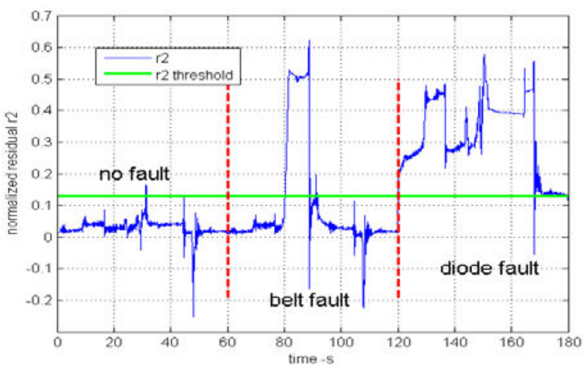

FIGURE 21. RESIDUAL R2.

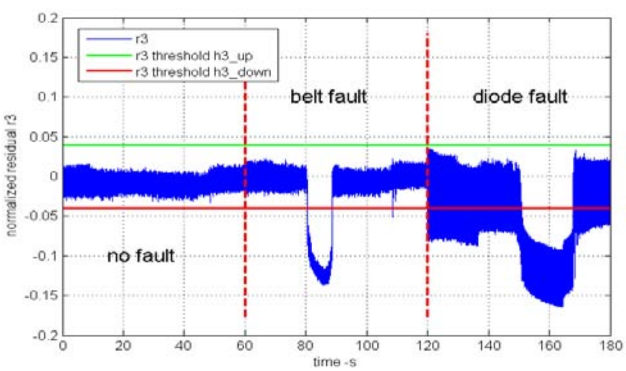

FIGURE 22. RESIDUAL R3.

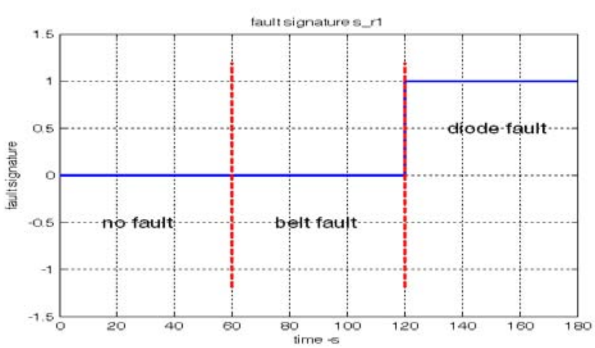

FIGURE 23. FAULT SIGNATURE S1.

ACKNOWLEDGMENTS

Authors would like to thank General Motors Corporation for the financial support and technical guidance as well as the staff at CAR for their assistance with the experiments.

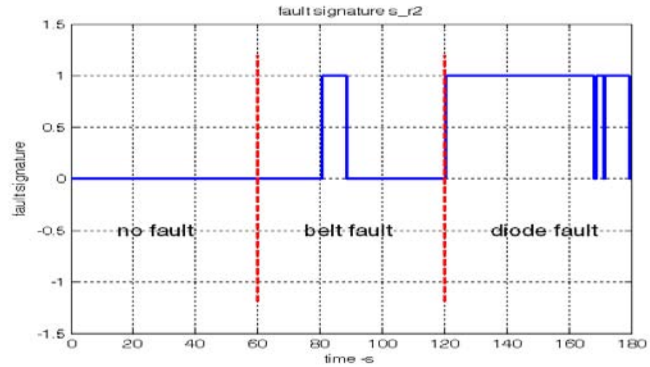

FIGURE 24. FAULT SIGNATURE S2.

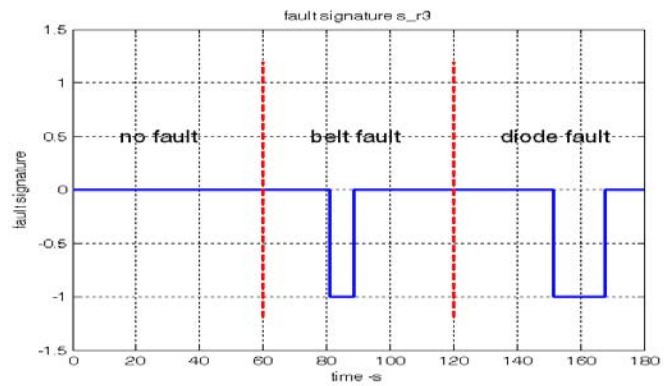

FIGURE 25. FAULT SIGNATURE S3.

REFERENCES

[1] De-Shiou Chen, *Sliding mode observers for automotive alternators*, Ph.D. Dissertation, The Ohio State University, 1998.

[2] Weiwu Li, *Model based fault diagnosis of automotive electric power generation system*, Master's Thesis, The Ohio State University, 2008.

[3] A. Scacchioli, G. Rizzoni, P. Pisu "Hierarchical model based fault diagnosis for an electrical power generation storage automotive system", *Proceedings of the American Control Conference*, New York City, NY, 2007.

[4] H. L. Van Trees, *Detection, Estimation, and Modulation Theory*, John Wiley and Sons, 1958.

[5] A. Scacchioli, G. Rizzoni, P. Pisu, "Model-Based Fault Diagnosis for an Electrical Automotive System", *Proceedings of the ASME International Mechanical Engineering Congress & Exposition,* Chicago, IL, 2006